

The influence of particle shape for granular media: A fourier-shape-descriptor-based micromechanical study

Z. Liu & J. Zhao

Hong Kong University of Science and Technology, Hong Kong

G. Mollon

Institut National des Sciences Appliquées de Lyon, France

ABSTRACT: Particle shape is known to affect the overall behavior of granular media significantly. It remains a great challenge to accurately characterize the shape of particles and incorporate its effects into the modeling of granular media in a quantifiable and verifiable manner. A micromechanical study based on 2D Discrete Element Method is presented in this paper to investigate the effect of particle shape irregularities on the granular responses. Novel in the study is the use of Fourier shape descriptors in the characterization of irregular particle shape based on statistical analysis of digital grain images obtained experimentally. We generate virtual irregularly and randomly shaped granular grains and introduce them into discrete element method for simulations of shear tests. The influences of irregular particle shape on the macroscopic stress-strain response, fabric anisotropy evolution, particle anti-rotation effect are carefully investigated and discussed. It is demonstrated that the shape effect has to be an important part in characterizing the micromechanics of granular media.

1 INTRODUCTION

The macroscopic response of a granular assembly is intrinsically controlled by the collective behavior of the constituent individual particles. Important particle level characteristics, such as particle size, shape characteristics, particle mineral composition and surface friction. Most natural occurring granular materials such as cohesion less sand usually have irregular shapes which play a crucial role in affecting the overall material responses. Numerous studies have revealed that macroscopic indexes such as the internal friction, shear strength, dilation and fabric evolution of granular media bear intimate relationship with the shape of the constituent particles (Rothenburg & Bathurst 1992; Matushima & Saomoto 2002; Cho et al. 2006; Azéma & Radjai 2012).

Particle-based methods such as Discrete Element Method (DEM) are widely employed to study the behavior of granular media from the particle level. While great convenience has been gained by the use of circle or sphere particles, they are far from accurate characterization of real sand particles. Other simple geometries such as polygon, ellipse and clusters of discs or spheres, have also been employed, but none of them can offer adequate characterization of the shape effect. A Fourier-shape-descriptor based method has recently been proposed by Mollon & Zhao (2012, 2013a) and Zhao & Mollon (2013) for generation

of real sand particles. In line with previous studies including Meloy (1977) and Bowman et al (2001), this method employs the Fourier shape descriptors derived from digital images of real sand to reconstruct the shape of sand particles and incorporate them into DEM simulation. Different from existing ways of shape characterization, such as those based on shape indices including sphericity, roundness, angularity and roughness, the use of Fourier descriptors renders it possible to quantify particle shape in a more systematic and accurate manner. It also lends convenience to characterize and reconstruct the shape of particles in a statistical and consistent way and meanwhile to account for the natural randomness in shape. The method had been applied to the modeling of granular hopper flow of Toyoura sand (Mollon & Zhao 2013b,c).

In this study, we employ the Fourier-shape-descriptor based method to generate virtual particles with random irregular shapes. Focus is placed here on the influence of one particular aspect of particle shape, the irregularity, on the overall response of the granular media. We investigate the macroscopic responses including the shear strength and volumetric behavior. The correlation of shear-induced anisotropy is also correlated to the degree of irregularity in particle shape for granular assemblies. How the presence of irregularity in particle shape contributes to the rolling resistance and interlocking of a granular assembly is also discussed.

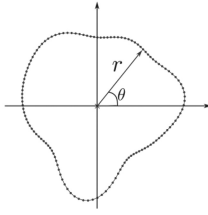


Figure 1. Illustration of contour discretization in polar coordination system.

2 METHODOLOGY

2.1 Characterization of particle shape by Fourier descriptors

The Fourier descriptors originally proposed Meloy (1977) and more recently employed by Mollon & Zhao (2012) are used to characterize the shape of sand particles. For a given shape contour of a 2D particle, the following normalized discrete Fourier spectrum for a given harmonic n is used as shape descriptor

$$D_n = \sqrt{A_n^2 + B_n^2} / r_0 \quad (1)$$

where A_n, B_n denote the discrete Fourier spectrum of the 2D shape contour discretized into N points in polar (r, θ) coordinates shown in Figure 1. r_0 is the average radius of all discrete contour points.

Following Mollon & Zhao (2012), 128 discrete points are chosen to describe the shape contour of a particle in this study, which leads to 64 effective harmonics modes denoted by 64 Fourier descriptors. The Fourier descriptors associated with different mode correspond to different aspects of particle shape property. Specifically, D_0 is always equal to 1 due to normalization. D_1 can be adjusted to 0 by choosing proper center of the particle. D_2 pertains to the elongation of the particle. D_3 to D_8 control the major irregularities of the shape contour. Those descriptors with mode number $n > 8$ may represent the surface roughness of the shape contour. With the aid of Fourier shape descriptors, we are able to investigate the peculiar influence of any of these shape characteristics on the overall material response. In the present study, we employ the following expression to construct different Fourier spectrums, placing an emphasis on the influence of D_3 to D_8 on the material behavior

$$\begin{aligned} D_2 &= 0 \\ D_n &= 2^{-2 \cdot \log_2(n/3) + \log_2(D_3)} \quad \text{for } 3 < n < 8 \\ D_n &= 0 \quad \text{for } 8 \leq n \leq 64 \end{aligned} \quad (2)$$

The interpolation function for modes $3 < n < 8$ has been adopted based on experimental data of Kahala beach sand and Toyoura sand provided by Das (2007). Based on Equation 2, the irregularities of the particle shape can be controlled by varying D_3 only. While they may be equally important, the effects of particle elongation and surface roughness will not be discussed in this study.

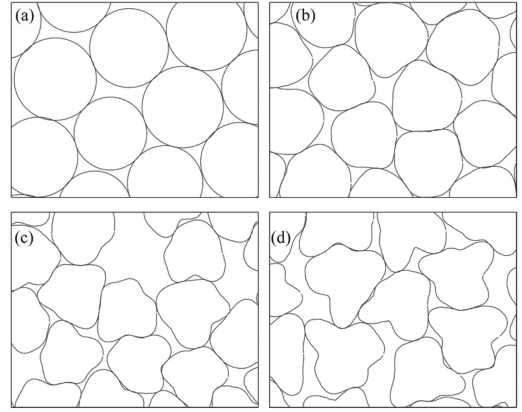


Figure 2. Irregular particles generated with (a) $D_3 = 0.00$ (disc), (b) $D_3 = 0.06$, (c) $D_3 = 0.12$ (d) $D_3 = 0.18$.

Given the Fourier shape spectrums, the discretized contour points of a complex shaped particle can then be constructed by

$$A_n = D_n \cdot \cos \delta_n \quad (3)$$

$$B_n = D_n \cdot \sin \delta_n \quad (4)$$

$$\bar{r}(\theta_i) = r_0 + \sum_{n=1}^N [A_n \cos(n\theta_i) + B_n \sin(n\theta_i)] \quad (N=64) \quad (5)$$

where δ_n is the phase angle defined as

$$\delta_n = \tan^{-1} \left(\frac{B_n}{A_n} \right) \quad (6)$$

δ_n is chosen randomly within the range of $[-\pi, \pi]$ following a uniform distribution for each individual mode, which may help to generate a group of particles of different shapes but with the same Fourier spectrums (e.g., the same sand). Figure 2 demonstrates examples of irregular particles with different D_3 . Notably, higher D_3 corresponds to more irregular shape particles, and accordingly, their shape appears to be more concave and/or convex. The D_3 values chosen in the present study are 0.02, 0.06, 0.12 and 0.18. The observation of 8 natural sands suggests a range of D_3 being around 0.036 ~ 0.1.

2.2 Sample preparation for DEM simulation

The granular assemblies comprised of complex shaped particles used for the subsequent DEM simulations are generated following the Fourier-Voronoi method presented by Mollon & Zhao (2012). Specifically, a squared domain is first treated by Voronoi tessellation. Each of the Voronoi cells is inserted a complex shape particle generated according to Section 2.1 where the particle center is made coincide with the Voronoi cell seed point. While the shape of each particle is determined by the Fourier descriptors, its orientation and

size are subject to constraints by the host cell. According to the procedure, granular samples containing 2000 to 2500 particles are prepared. The radii of particles in each sample range from 6.0 mm to 7.0 mm. While the particles in each sample are randomly distributed, the generated sample is initially isotropic.

Due to the complex shape of particles, there may be multiple contacts between two particles. To implement the generated assemblies into DEM simulation, the ODEC method is employed in this paper (Ferrellec & McDowell, 2008; Mollon & Zhao, 2012). In the ODEC method, each complex-shape particle is simulated by a rigid cluster of certain number of circles with various radiuses. The circles are chosen to best fit the particle contour and satisfy the shape characterization. A simple linear spring-dashpot contact model in conjunction with Coulomb's friction law are then used to describe the contact between two constituent disks of two contacted particles.

After implemented into DEM simulation, the granular assemblies are then isotropically compressed until the desired confining pressure and equilibrium state are reached. The initial confining pressure in the present study is set to be 1MPa. The inter-particle friction coefficient μ is set to be 0 during the consolidation stage and is then fixed at 0.5 during the shearing loading for all the samples. Relatively dense and homogeneous samples are prepared after consolidation. A shear rate of 5%/s is then applied to the samples in the vertical direction while horizontal confining stress is kept constant. Periodic boundaries are used to maintain the packing homogeneity. The stiffness of the contact spring is set to be $k_n = 4 \times 10^8 N/m$ and $k_t/k_n = 0.75$ where k_n and k_t denote the normal and tangential stiffness, respectively. Both inter-particle dashpot and global non-viscous damping are applied to accelerate the convergence of the molecular dynamics simulation towards the equilibrium state to maintain the quasi-static condition. The shear process is continued until the sample reaches a steady state of constant volume and mean normal stress.

3 RESULTS AND ANALYSIS

3.1 Macroscopic responses

Figure 3 presents the evolution of shear stress ratio q/p and the volumetric strain ε_v with the axial strain for different value of D_3 . In all four cases, the shear stress shows a peak followed by a softening stage until the residual state is reached. All samples also experience instant contraction first and then continuous dilation. The overall behavior appears to match that of a dense sand. Under monotonic shear, the samples with higher D_3 exhibit relatively higher peak strength. Compared to the smooth disc particle case, samples with irregular particles show a stiffer elastic modulus. Apparently, when densely packed irregularly shaped particles are compressed, their irregular shape easily causes interlocking among themselves which prohibits their mobility at relatively small strain level. This gives

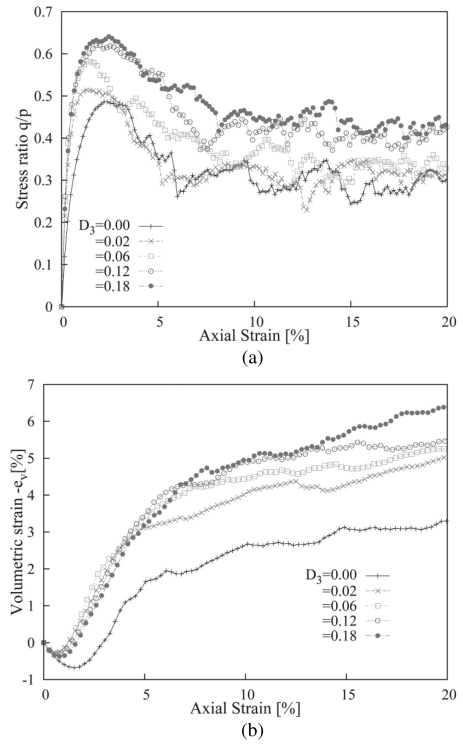


Figure 3. Macroscopic response of granular packings under shear (a) stress ratio evolution, (b) volumetric strain evolution.

rises to their enhanced elastic stiffness as compared to the circular particle case. Meanwhile, it is observed the increase of D_3 may lead to more significant initial contraction and enhanced dilation at late stage, as well as increased residual shear strength.

3.2 Stress-induced anisotropy

Shear may induce anisotropy for an initially isotropic sample (Guo & Zhao, 2013; Zhao & Guo, 2013). In this section, we analyze the stress-induced anisotropy of the different samples to identify the correlation between the shape irregularity and the shear induced anisotropy. We follow the definition of fabric tensor proposed by Satake (1982) to quantify the contact normal distribution in a granular packing

$$\phi_{ij} = \int_0^{2\pi} E(\theta) n_i n_j d\theta = \frac{1}{N_c} \sum_{c \in N_c} n_i n_j \quad (7)$$

where n_i represents the unit vector of the contact normal direction and $E(\theta)$ is the probability density function of contact normal in terms of direction. A second-order Fourier expansion of $E(\theta)$ is employed to approximate the contact normal distribution

$$E(\theta) = \frac{1}{2\pi} (1 + a_{ij}^c n_i n_j) = \frac{1}{2\pi} [1 + a_c \cos 2(\theta - \theta_c)] \quad (8)$$

where the fabric anisotropy can be expressed as

$$a_{ij}^c = 4\phi_{ij}' \quad (9)$$

where ϕ_{ij}' is the deviatoric part of ϕ_{ij} . a_c is the deviatoric invariant of fabric tensor ϕ_{ij} and is usually used to quantify the degree of anisotropy. θ_c is the principal direction of the contact normal. Similar definition is employed for the mechanical anisotropy including both normal and shear component according to Rothenburg (1980). The distribution of average contact force by direction can be expressed as

$$\bar{f}^n(\theta) = \bar{f}^0 [1 + a_n \cos 2(\theta - \theta_n)] \quad (10)$$

$$\bar{f}^t(\theta) = \bar{f}^0 a_t \sin 2(\theta - \theta_t) \quad (11)$$

where \bar{f}^0 is the average normal contact force calculated over all directions with the same weight and may not be equal to the average normal contact force over all contacts

$$\bar{f}^0 = \int_0^{2\pi} \bar{f}^n(\theta) d\theta \quad (12)$$

a_n and a_t are then used to quantify the normal and shear force anisotropy, respectively.

Figure 4 shows the evolution of a_c , a_n and a_t of the four samples with irregular shape particles under monotonic shear. In all cases, both a_c and a_t depict a peak and then decreases to a residual state. A sample with higher D_3 generally shows a marginally higher contact normal anisotropy a_c , while the enhancement is quite apparent in the case of a_t . The smaller D_3 case appears to attain a peak of a_t at a slightly smaller strain level. In contrast, the peak of a_n becomes lower with the increase in D_3 . In addition, a lower residual strength is found for the case with a smaller for both a_c and a_t , whereas for a_n it stays roughly the same for all cases. Further examination of the contact level information reveals that the increase in particle irregularity generally leads to decreased number of contact in the lateral supporting direction (to the major shear direction) where relatively higher contact normal forces are concentrated, which results in more homogeneous anisotropy behavior for a_n and accounts for its drop of in peak with the increase in D_3 .

We further validate the following stress-force-fabric relationship proposed in Rothenburg (1980) in consideration of particle irregularity

$$\frac{q}{p} = \frac{1}{2}(a_c + a_n + a_t) \quad (13)$$

We choose the case $D_3 = 0.06$ as a demonstration example and the results are presented in Figure 5. As it can be seen, the analytical relationship coincides well with the DEM simulated data on the stress ratio. In particular, an inspection of the relative contribution of each source of anisotropy, it is found that the enhancement of shear strength by particle irregularity is mainly due to the increase in the shear force anisotropy (e.g., $a_n + a_t$) rather than the fabric anisotropy. The contribution of the normal force anisotropy a_n however reduces for more irregular shape cases. In addition, a_c and a_t jointly contribute to the increase in the residual strength.

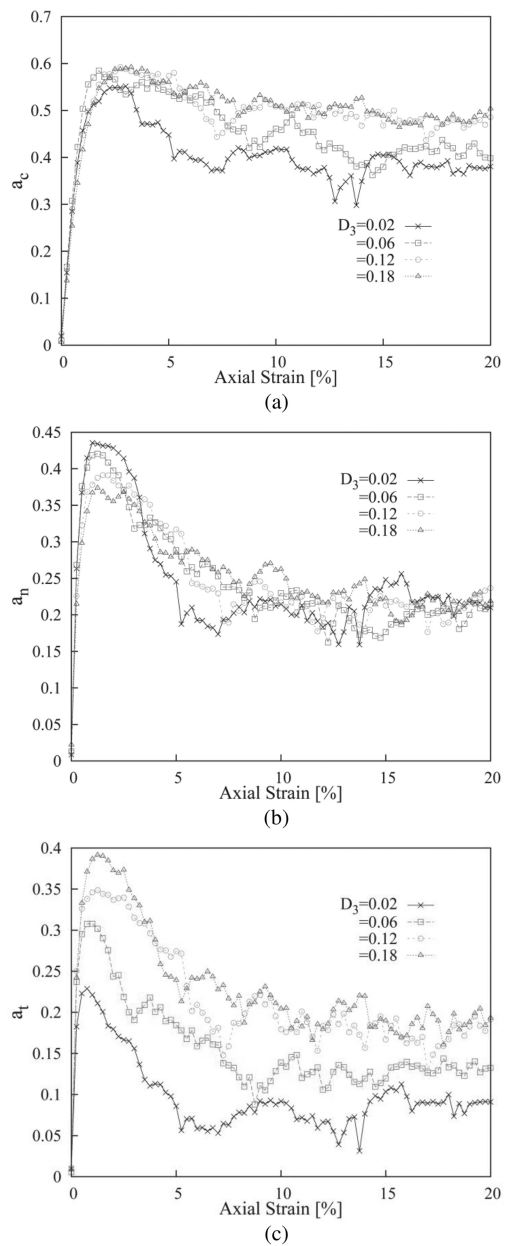


Figure 4. Evolution of shear induced anisotropy (a) contact normal anisotropy, (b) normal contact force anisotropy, (c) shear contact force anisotropy.

3.3 Rolling resistance by irregular particles

Unlike in a disk case where only single contact exists between particles, the consideration of irregular particle shape renders multiple contacts between contacted particles become common. This may further lead to hindering of relative rotation movement and

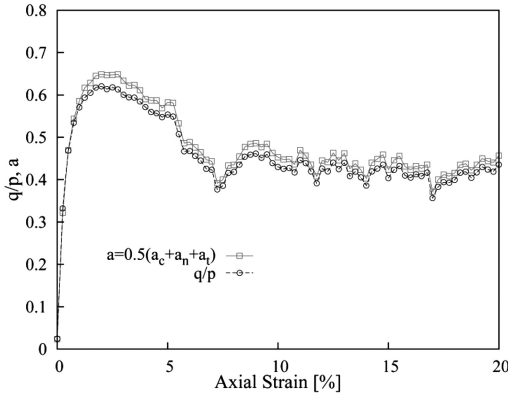


Figure 5. Verification of stress-force-fabric relationship in Equation 13 by the DEM results using irregular particles.

thus rolling resistance. An alternative way to quantify the rolling resistance effect is to investigate the ‘blocking moment’ of a particle defined below

$$M_b = \frac{1}{N_p} \sum_i \left(\frac{\sum_{c \in N_i^c} \vec{r}_i^c \times \vec{f}_{ni}^c}{\sum_{c \in N_i^c} r_i^c f_{ni}^c} \right) \quad (14)$$

where M_b is the mobilized average blocking moment of the packing. N_p is the number of particles. N_i^c is the number of contacts on particle i . Figure 6 presents a schematic illustration of M_b . M_b indeed represents the moment provided by the normal forces at each contact surrounding the considered particle with respect to its centroid. According to Tordessillas (2009), this moment is most mobilized between particles in forming the force chains and is released with the force chains buckle. To certain extent it reflects the degree of granular jamming. In our study it is further normalized with the volume weight of particle stress provided by the normal contact force σ_m^n

$$\sum_{c \in N_i^c} r_i^c f_{ni}^c = V_p \sigma_m^n \quad (15)$$

where V_p is the volume of the particle. The stress is similar to the ‘load vector’ (Tordessillas, 2009) whose magnitude depends on the force chain penetrating through the particle. For irregularly shaped particles, the concave or convex parts of the surface may offer perfect conditions of interlocking with its neighboring particles to provide rolling resistance in force chain buckling.

Figure 7 shows the evolution of M_b for different samples during the shearing process. Notably in all cases, M_b is mobilized quickly within a small range of shear strain (termed as peak strain hereafter) before reaching a steady magnitude and stays at that level for the rest of the shearing course. A correlation with the volumetric change curve in Figure 3b indicates the peak strain level for M_b coincides with the phase transformation strain marking the contraction to dilation transition in a sample. It is evident that the instant

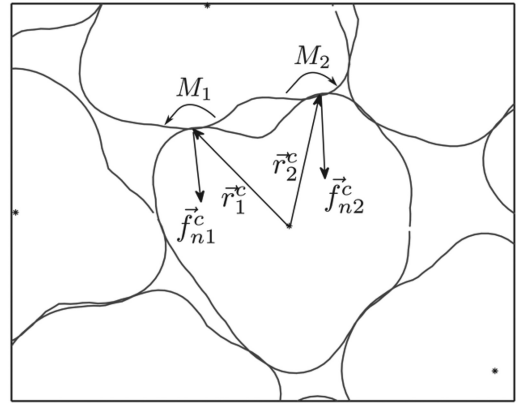


Figure 6. Illustration of ‘blocking moment’ offered by inter-particle normal contact force which leads to rolling resistance.

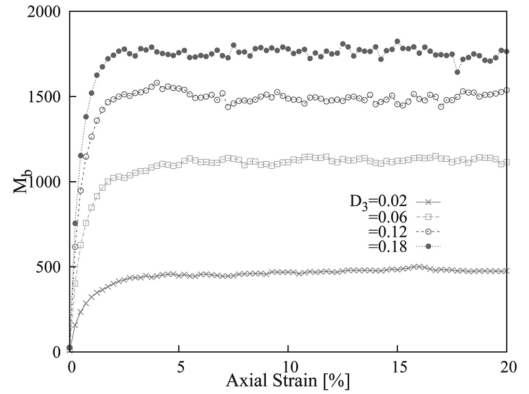


Figure 7. Comparison of mobilized average blocking moment between different shaped particles.

contraction of the sample when it is subject to external shear is the major mobilizer of the ‘blocking moment’. This value somehow does not drop when the sample enters dilative stage later on but stay at a constant value, indicating a relatively stable state where the formation and buckling of force chain approximately reaches equilibrium. It is also apparent that higher irregularity leads to higher M_b value. The reason is self-explanatory.

Figure 8 presents the mean rotation mobility defined as follows

$$\theta = \sqrt{\frac{\sum_i \Delta\theta_i^2}{N_p}} \quad (16)$$

where $\Delta\theta_i$ is the accumulative rotation angle of particle i and N_p is the number of particles. Higher θ indicates more accumulation of particle rotation in the sample. As clearly shown in Figure 8, as the particles become more irregular, they are less rotation-active due to increased interlocking among particles.

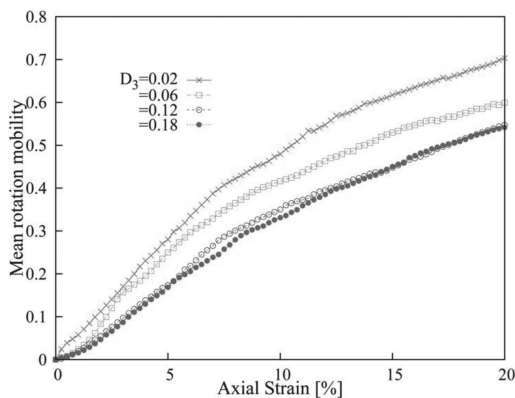


Figure 8. Evolution of the mean rotation mobility of different shaped particles.

4 CONCLUSION

The influence of one aspect of particle shape, irregularity, on the overall mechanical behavior of granular media was investigated. We employed the approach based on Fourier shape descriptors to generate irregularly shaped particles and then packed them into a sample using Fourier-Voronoi approach for the subsequent DEM simulation. The Fourier shape descriptor approach provides a feasible and quantifiable way on shape characterization. This was demonstrated by selecting the Fourier shape descriptor D_3 , which characterizes the irregularity of particle shape, for the study. Its influence on the drained behavior of a sheared granular assembly with varied degree of irregularity was thoroughly investigated.

The DEM results showed that the irregularity in shape of the constituent particles may help to enhance the shear strength and the dilatancy of a granular material. It may lead to more intense instantaneous contraction and enhanced dilation in the volumetric change. A packing with irregular shape particles also show an overall stiffer elastic modulus than one containing smooth disc particles. The strength increase in the irregularly-shaped particle case is mainly due to the increase of shear force anisotropy. The irregular shape tends to prohibit the relative rotation among particles and leads to macroscopic interlocking.

REFERENCES

Azéma, E. & Radjai, F. 2012. Force chains and contact network topology in sheared packings of elongated particles. *Phys. Rev. E*. 85.031303.

Bowman, E. T., Soga, K. & Drummond, W. (2001). Particle shape characterization using Fourier descriptor analysis. *Geotechnique* 51(2): 545–554.

Cho, G., Dodds, J. & Santamarina, J.C. 2006. Particle shape effects on packing density, stiffness, and strength: natural and crushed sand. *J. Geotech. Geoenviron. Eng.* 132(5): 591–602.

Das, N. 2007. Modeling three-dimensional shape of sand grains using discrete element method. PhD Thesis. University of South Florida, Florida, USA

Ferrellec, J.-F. & McDowell, G.R. 2008. A simple method to create complex particle shapes for DEM. *Geomech. Geoenng* 3(3): 211–216.

Guo, N. & Zhao, J. D. 2013. The signature of shear-induced anisotropy in granular media. *Computers & Geotechnics* 47:1–15.

Matsushima, T. & Saomoto H.2002. Discrete Element Modeling for Irregularly-shaped Sand Grains. In Mestat (ed.), *Numerical Methods in Micromechanics via Particle Methods: international PFC Symposium, Gelsenkiren, Germany, Nov 2002*.

Meloy, T.P. 1977. Fast Fourier transform applied to shape analysis of particle silhouettes to obtain morphological data. *Powder Technol* 17: 27–35.

Mollon, G. & Zhao, J. D. 2012. Fourier-Voronoi-based generation of realistic samples for discrete modeling of granular materials, *Granular Matter* 14(5): 621–638.

Mollon, G. & Zhao, J. D. 2013a. Generating realistic 3D sand particles using Fourier Descriptors. *Granular Matter* 15(1): 95–108.

Mollon, G. & Zhao, J.D. 2013b. Characterization of fluctuations in granular hopper flow. *Granular Matter* 15(2): 827–840.

Mollon, G. & Zhao, J.D. (2013c). The influence of particle shape on granular Hopper flow. *AIP Conference Proceedings* 1542: 690–693.

Rothenburg L. 1980. Micromechanics of idealized granular systems. Ph.D. thesis, Carleton University, Ottawa, Ontario, Canada.

Rothenburg, L. & Bathurst, R. J. 1992. Micromechanical features of granular assemblies with planar elliptical particles. *Geotechnique* 42(1): 79–95.

Satake M. 1982. The role of the characteristic line in static soil behavior. In BalkemaAA (ed). *IUTAM symposium on deformation and failure of granular materials*, Delft.

Todessillas, A. 2009. Force chain buckling, unjamming transitions and shear banding in dense granular assemblies, *Philosophical Magazine* 87(32): 4985–5016.

Zhao, J. D. & Guo, N. 2013. Unique critical state characteristics in granular media considering fabric anisotropy. *Geotechnique* 63(4): 695–704.

Zhao, J. D. & Mollon, G. (2013). A Statistically-based Approach on Reconstructing Sand Particles for Discrete Modeling. *Proceedings of the Workshop on Experimental Micromechanics for Geomaterials*, Hong Kong, May 2013.